PNAS RESEARCH ARTICLE | EARTH, ATMOSPHERIC, AND PLANETARY SCIENCES

More extensive land loss expected on coastal deltas due to rivers jumping course during sea-level rise

Austin J. Chadwick[a,1], Sarah Steele[a], Jose Silvestre[a], and Michael P. Lamb[a]

Edited by Andrea Rinaldo, Ecole Polytechnique Federale de Lausanne, Lausanne, Switzerland; received October 22, 2021; accepted June 9, 2022

River deltas are home to hundreds of millions of people worldwide and are in danger of sinking due to anthropogenic sea-level rise, land subsidence, and reduced sediment supply. Land loss is commonly forecast by averaging river sediment supply across the entire delta plain to assess whether deposition can keep pace with sea-level rise. However, land loss and deposition vary across the landscape because rivers periodically jump course, rerouting sediment to distinct subregions called delta lobes. Here, we developed a model to forecast land loss that resolves delta lobes and tested the model against a scaled laboratory experiment. Both the model and the experiment show that rivers build land on the active lobe, but the delta incurs gradual land loss on inactive lobes that are cut off from sediment after the river abandons course. The result is a band of terrain along the coast that is usually drowned but is nonetheless a sink for sediment when the lobe is active, leaving less of the total sediment supply available to maintain persistent dry land. Land loss is expected to be more extensive than predicted by classical delta-plain–averaged models. Estimates for eight large deltas worldwide suggest that roughly half of the riverine sediment supply is delivered to terrain that undergoes long periods of submergence. These results draw the sustainability of deltas further into question and provide a framework to plan engineered diversions at a pace that will mitigate land loss in the face of rising sea levels.

land loss | sea-level rise | river deltas | river avulsions | river diversions

Significance

Deltaic land is valuable and at risk of drowning due to relative sea-level rise. Forecasts for the next century suggest sediment deposition by rivers can help counteract land loss, but estimates have yet to account for deposition patterns as rivers change course over time. We present a model and a laboratory experiment that resolve these patterns. Results show deltaic land is in more danger than previously anticipated. Repeated changes in river course temporarily build land that later drowns for decades to centuries. This process leaves less of the river's sediment supply available to sustain persistently dry and habitable land. Revised forecasts suggest deltas worldwide will require more sediment—or frequent engineered river diversions—to sustain land through the coming century.

River deltas host natural resources, ecosystem services, and coastal megacities home to over 300 million people worldwide (1, 2). Because deltaic plains are maintained by sediment deposition in areas at or near sea level, they are vulnerable to land loss as sea level rises (Fig. 1*A*) (3, 4). Anthropogenic interference is endangering deltas worldwide: climate change drives global sea-level rise at an accelerating pace (5), groundwater and hydrocarbon extraction induce coastal subsidence (6), and dams and levees restrict the deposition of sediment (7, 8). These pressures are escalating globally, and projections for land loss in the coming century are dire (1, 9, 10).

Land-loss projections are commonly based on sediment-mass-balance models averaged over the entire landscape (3, 10–14). Rivers supply sediment to deltas at a volumetric rate (Q_s) that is partitioned between vertically accreting the delta plain at the rate of relative sea-level rise (σ) and laterally expanding the delta-plain area (A),

$$\frac{Q_s}{c_0} = A\sigma + H_b\frac{dA}{dt}, \quad [1]$$

where H_b is the basin depth offshore and c_0 is the solids fraction in the sediment deposit (1 − porosity) (Fig. 1*B*) (13, 14). Eq. **1** does not consider additional offshore and biogenic sources of sediment (15–17) or wave erosion (18, 19) for simplicity. Given projected rise rates, many densely populated deltas do not have enough sediment to sustain their current area (10). To sustain their current area ($\frac{dA}{dt} = 0$), rivers need at least enough sediment to vertically accrete the delta-plain area at pace with sea-level rise,

$$Q_{s,need} = c_0 A\sigma, \quad [2]$$

where $Q_{s,need}$ is the needed sediment supply (13, 14).

These landscape-averaged models are based on the simplifying assumption that rivers evenly distribute sediment across the delta plain. However, coastal rivers typically partition sediment intermittently among four to six subregions called delta lobes (Fig.1*C*) (18, 20, 21). Sediment supply is primarily deposited on the lobe hosting the active river channel. Other lobes may remain inactive—without their main supply of riverine sediment—for tens to thousands of years (Fig. 1*C*). Deposition shifts to a new lobe when the river jumps course, in naturally occurring river diversions called avulsions (22).

Author affiliations: [a]Division of Geological and Planetary Sciences, California Institute of Technology, Pasadena, CA 91125

Author contributions: A.J.C. and M.P.L. designed research; A.J.C., S.S., J.S., and M.P.L. performed research; A.J.C., S.S., J.S., and M.P.L. analyzed data; and A.J.C., S.S., J.S., and M.P.L. wrote the paper.

The authors declare no competing interest.

This article is a PNAS Direct Submission.

[1]To whom correspondence may be addressed. Email: austin.chadwick23@gmail.com.

This article contains supporting information online at http://www.pnas.org/lookup/suppl/doi:10.1073/pnas.2119333119/-/DCSupplemental.

Published July 25, 2022.

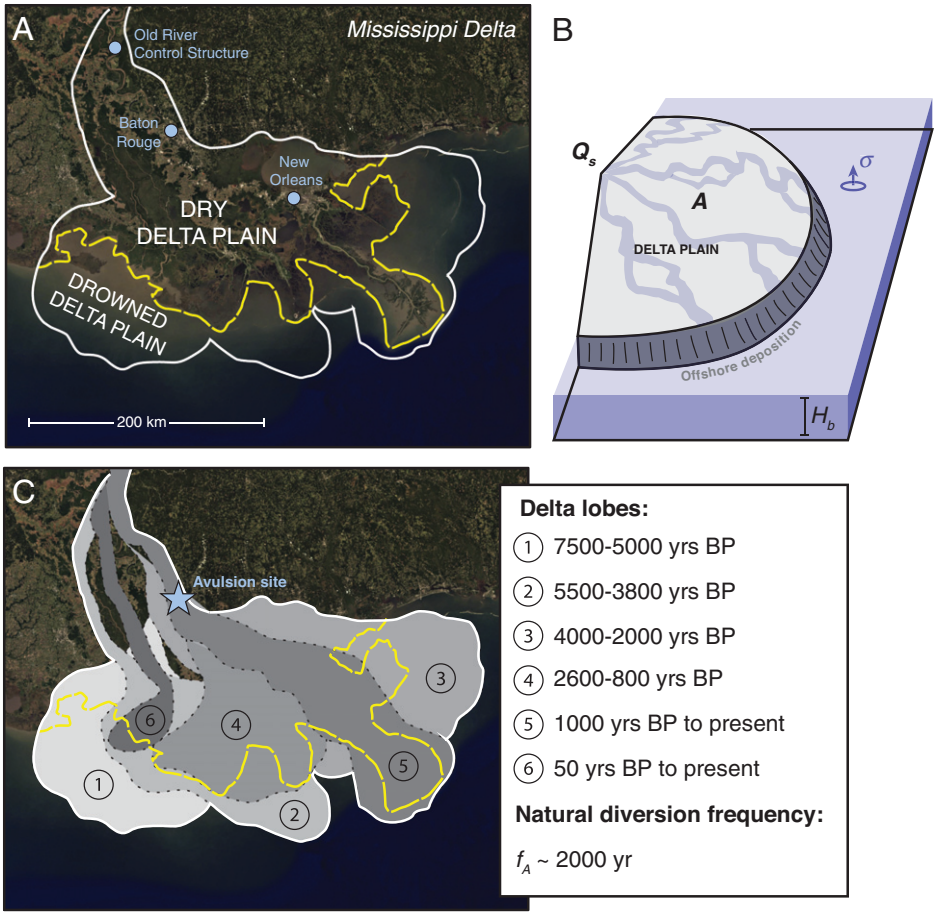

Fig. 1. (*A*) Satellite view of the Mississippi River delta (Google Earth) outlining the delta plain (white line) (21) and the modern shoreline (dashed yellow line) (51), which is retreating due to relative sea-level rise. (*B*) Definition sketch of a landscape-averaged model (Eqs. **1** and **2**). (*C*) Same as *A*, here showing that the delta plain is composed of multiple lobes (gray-shaded regions bounded by dotted lines). Each lobe was built by a different path of the Mississippi River, which has naturally diverted its course every 2,000 y (see *Inset*). The drowned delta plain is primarily found along older, inactive delta lobes.

Avulsions are abrupt, reoccurring events—like earthquakes—with a characteristic frequency that varies from delta to delta (23). For instance, avulsions on the Mississippi River have occurred every 2,000 y (21) (Fig. 1*C*), whereas avulsions on the Yellow River have taken place every decade (20, 24).

River avulsions are important for building new land and sustaining existing land in the face of relative sea-level rise (25). At the same time, avulsions necessarily involve abandonment of the old lobe, leaving it deprived of sediment and vulnerable to land loss (26). The implications are unclear: Land losses and gains among lobes could have an unforeseen impact on delta-plain evolution, or alternatively losses and gains could potentially compensate one another such that the delta plain evolves according to landscape-averaged models. Regardless, land loss on inactive lobes could persist for centuries (Fig. 1*C*), rendering coastal zones effectively uninhabitable.

Engineering on some deltas has eliminated avulsions altogether through dams and levees (27). Anthropogenic interference has come at a high cost: many delta lobes are now permanently cut off from their source of sediment, resulting in catastrophic land loss (8, 26). Ongoing billion-dollar efforts aim to restore natural avulsion benefits through engineered diversions (11, 25, 28), which may reroute the river completely (e.g., the Yellow River Delta) (25, 26, 29) or partially (e.g., the 1963 Atchafalaya diversion of the Mississippi River at the Old River Control Structure; Fig. 1*A*) (30–32). Coastal management leaders face decisions regarding when and where diversions should be made and where land can be intentionally left to drown (11, 27). Some efforts have proven successful (31, 33), and scientists agree that multiple large-scale diversions are so effective at combating land loss that the question is not if, but rather how, such diversions will be implemented in the future (11, 12, 34). A predictive framework is needed to understand the extent to which diversions can restore sinking land and how diversions should be implemented to maximize the land-building potential of sediment resources.

Whether through natural avulsions or engineered diversions, the cycles of sediment delivery among lobes determine where coastal land is built and where it is lost. Here, we present a model to forecast land loss that accounts for river avulsion among lobes. We then validate the model against a scaled laboratory experiment, and we compare how its predictions for future land loss on densely populated deltas differ from that of classical landscape-averaged models.

Accounting for Avulsions and Delta Lobes in Land-Loss Forecasts

Landscape-averaged models (Eqs. **1** and **2**) are based on the idea that a river evenly distributes its sediment supply across the subaerial delta plain. Model forecasts can be improved by accounting for potential land loss on inactive delta lobes due to intermittent sediment delivery. Rivers build land on the active delta lobe, but after avulsion, the majority of the sediment supply is diverted elsewhere and some of this land will be lost as sea level rises. Lost land may be rebuilt during the later reoccupation of the delta lobe, but lobes spend most of their time

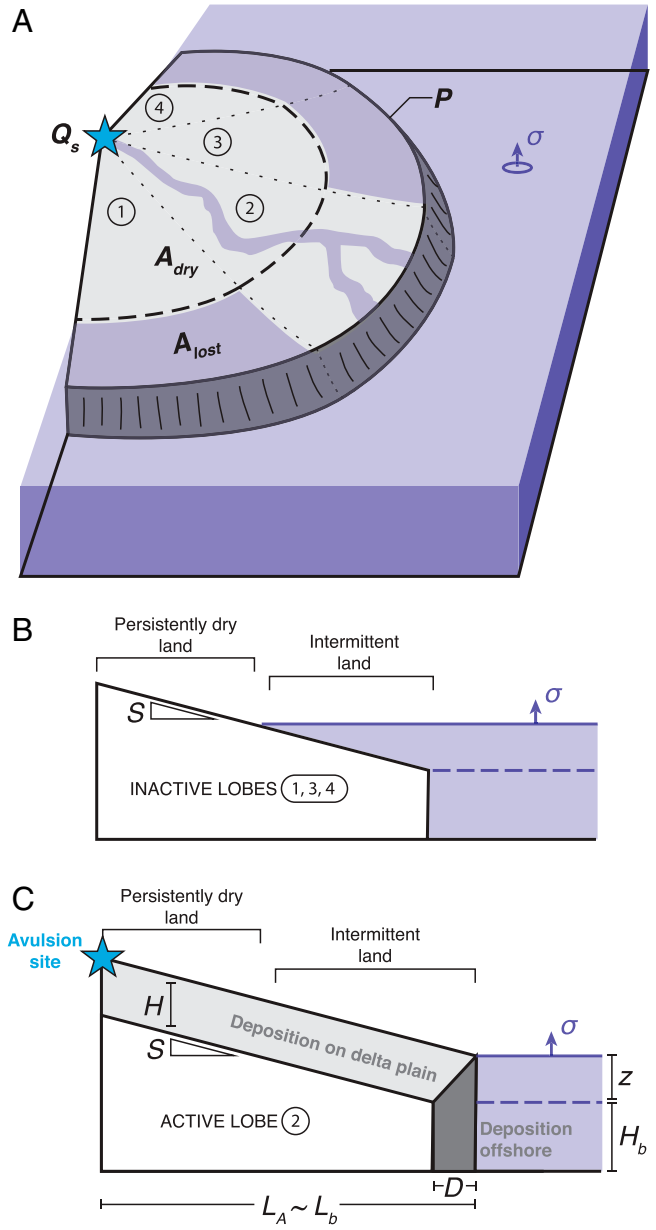

Fig. 2. (*A*) Definition sketch of the lobe-averaged model (*SI Appendix*, Eqs. S3–S5) for a delta with four lobes delineated by dotted lines. The dashed line shows the upstream extent of intermittent land, which is gradually lost during lobe inactivity and periodically regained when a lobe is reactivated. (*B*) Cross-section view of an inactive lobe where sea-level rise causes intermittent land loss (Eq. **4**). (*C*) Cross-section view of an active lobe, where the river deposits sediment on both persistent and intermittent land (Eq. **5**).

inactive and thus partially drowned (Fig. 2*A*). To account for drowning on inactive lobes, the total delta-plain area (A in Eq. **1**) should be subdivided into the intermittent land area that is gradually lost during lobe inactivity (A_{lost}) and the persistent land area that remains dry regardless of lobe state (A_{dry}),

$$A_{dry} = A - A_{lost}. \quad [3]$$

Intermittent land area is approximated by a band of terrain along the coastal perimeter (P) that progresses landward where lobes are inactive (Fig. 2*A*). For simplicity, we estimate a characteristic perimeter by the square root of the dry delta-plain area ($P = \sqrt{A_{dry}}$) (13), which should hold for a variety of delta symmetries and basin geometries, and we adopt a characteristic seaward slope S for all lobes. Furthermore, we assume inactive lobes are completely deprived of sediment and do not consider additional sources of sediment (15–17) or erosion (18, 19). Inactive lobes passively drown as the shoreline retreats at a velocity given by the ratio of the rise rate and the seaward slope (σ/S; Fig. 2*B*). The intermittent land area is determined by integrating shoreline retreat velocity across the coastal perimeter until a given lobe is reactivated,

$$A_{lost} = \left(\frac{\sigma}{S}P\right)\frac{n}{f_A}, \quad [4]$$

where the term in parentheses is the rate of land loss on inactive lobes and the second term is the average time before avulsions reroute the river back to the same lobe, where f_A is the avulsion frequency, $n = \frac{N+1}{2}$, and N is the number of lobes (35).

Previous work shows f_A scales inversely with the time it takes the river to deposit sediment to a thickness comparable to the river channel depth (H_c) on the active-lobe delta plain; at this point, flow in the channel is rendered gravitationally unstable, and overbank floods can trigger avulsion (22, 24, 36). Avulsion frequency can be estimated by sediment mass balance, similar to Eq. **1** but here averaged across a delta lobe (Fig. 2*C*) (37),

$$\frac{Q_s}{c_0} = f_A\left(L_A - \frac{1}{2}D\right)BH + f_A DB\left(H_b + \frac{1}{2}z\right), \quad [5]$$

where the first term on the right-hand-side represents sediment deposition on the delta plain and the second term represents offshore deposition; $z = n\sigma f_A^{-1}$ is the height of sea-level rise before a lobe is reactivated; $D = \frac{(H-z)}{S}\mathcal{H}\left(\frac{H-z}{S}\right)$ is the nonnegative distance the active lobe builds seaward (where $\mathcal{H}$ is the Heaviside step function); and H and B are the active lobe's thickness and width of deposition. The lobe length is the avulsion length L_A, i.e., the distance up-river from the sea where avulsions occur (Fig. 2*C*). On lowland deltas, L_A can extend hundreds of kilometers up-river to a distance approximately equal to the backwater length-scale, $L_b \equiv H_c/S$ (23, 38). Together, Eqs. **3**–**5**. provide a means to forecast land loss that resolves intermittent sediment delivery due to switching of the active lobe.

Land Loss on an Experimental Delta

To test the landscape-averaged and lobe-averaged models, we conducted a scaled laboratory experiment. The experiment consisted of a 7-m-long, 14-cm-wide fixed-width flume connected to a 5-m-long, 3-m-wide ocean basin (Fig. 3*A* and *B*). Water and sediment were supplied at the upstream end, and sea level was controlled using a programmable standpipe at the downstream end. The basin was initially 4.5 cm deep and free of sediment, and over the course of 105 h, water flow naturally built a river delta. We designed the experiment to replicate realistic backwater-scaled avulsions ($L_A \sim L_b$) over length scales of ~1 m, achieved by oscillating input water and sediment supply such that the river experienced persistent backwater effects (39) while maintaining subcritical flow ($Fr < 1$), channel depths of $H_c = 7.5$ mm, and gentle bed slopes of $S = 0.0042$ ($L_b = H_c/S = 1.8$ m; *SI Appendix*, Table S1). We systematically raised sea level at four different speeds during four phases of the experiment, lettered A to D (Fig. 3*C*). Sea-level rise rates were scaled in terms of a dimensionless sea-level rise rate,

$$\sigma^* = \frac{\sigma}{Q_s/nL_bBc_0}, \quad [6]$$

where the denominator represents the maximum possible deposition rate averaged across the active-lobe delta plain. Rise rates

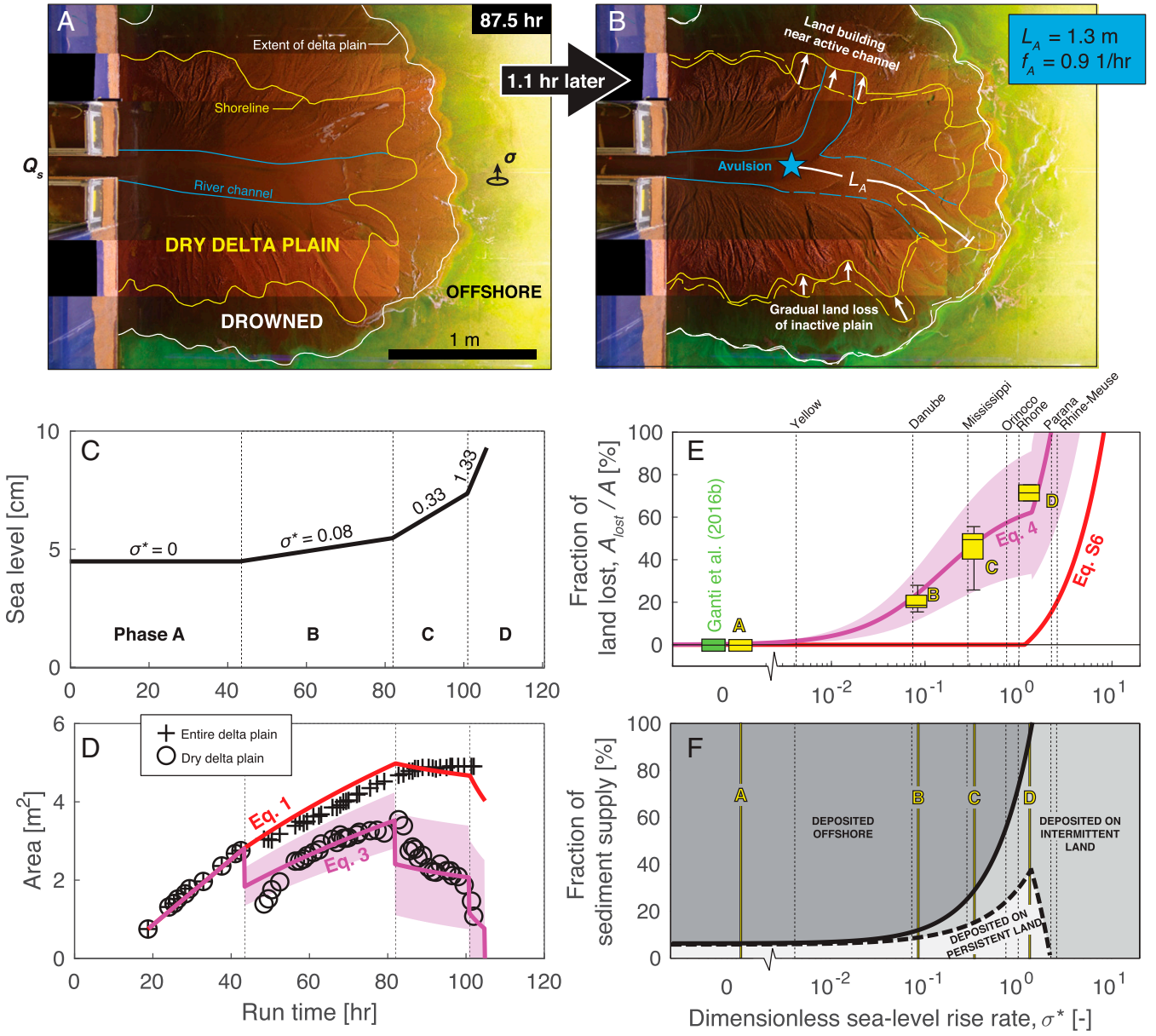

Fig. 3. Land loss on an experimental delta. (*A*) Overhead photograph showing mapped shoreline (yellow line) and delta-plain extent (white line) defining the dry and drowned delta-plain areas at 87.5 h. The river channel is labeled in blue. (*B*) Overhead photograph captured 1.1 h later, showing mapped avulsion (blue star) and measured avulsion length L_A and frequency f_A. Dashed lines show the shoreline and delta-plain extent from *A*, and white arrows highlight land building near the active channel and gradual land loss on inactive plains. (*C*) Sea-level curve for the experiment, showing labeled Phases A through D. (*D*) Area of the entire delta plain (crosses) and the dry delta plain (circles) over the experiment, alongside predictions from the landscape-averaged model (Eq. **1**) and the lobe-averaged model (Eq. **3**), with the shaded envelope showing propagated uncertainty from Eqs. **4** and **5**. (*E*) Drowned fraction of the delta plain as a function of dimensionless rise rate σ^* (Eq. **6**), showing experimental results (yellow box plots) and predictions from the landscape-averaged model (red; *SI Appendix*, Eq. **S6**) and lobe-averaged model (magenta; Eq. **4**). The magenta-shaded envelope shows propagated uncertainty in the predicted avulsion frequency (Eq. **5**). Dotted lines show σ^* values for deltas in nature (37). (*F*) Lobe-averaged model predictions for how dimensionless sea-level rise σ^* affects sediment partitioning between the persistently dry delta plain (light gray), the intermittently drowned delta plain (medium gray), and farther offshore (dark gray) (*SI Appendix*). The landscape-averaged model (Eq. **1**) does not differentiate between persistent and intermittent delta plain.

covered the range $0 < \sigma^* < 1$ common to natural deltas (37, 40). To isolate the effect of sea-level rise and river avulsions from other factors that influence land loss, the experiment featured no ocean waves, tides, storms, vegetation, or cohesive sediment (17, 41, 42). Overhead images were collected every minute of the experiment and used to map the area of dry and drowned land and identify avulsions (Fig. 3*A* and *B*; *Materials and Methods*).

The experimental delta evolved through repeated river avulsions (Fig. 3*A* and *B*). Without sea-level rise (Phase A; $\sigma^* = 0$; Fig. 3*C*), there was no land loss; the entire delta plain was persistently dry (Fig. 3*D* and *E*). Land area gradually increased at a rate of ~840 cm^2/h, in close agreement to models averaged over both the landscape (Eq. **1** in Fig. 3*D*) and lobe (Eq. **3** in Fig. 3*D*). Avulsions occurred once per 2 h on average ($f_A = 0.5$ [0.2, 1.0] h^{-1}, where terms in brackets represent the maximum and minimum; *SI Appendix*, Table S2) and focused land-building near the active river mouth.

With the onset of sea-level rise (Phase B; $\sigma^* = 0.08$; Fig. 3*C*), the delta plain lost land in inactive areas cut off from the riverine sediment supply (Fig. 3*A* and *B*). Inactive coastlines retreated by ~20 cm, forming a band of drowned terrain along the coast. The shape of the drowned zone varied over time depending on local slopes (43) and the time since an area was last supplied with

riverine sediment, and maintained a roughly constant size of ~0.9 m^2, which was ~25% of the entire delta plain (Fig. 3*E*). Avulsions were more frequent ($f_A = 0.9$ [0.2, 1.8] h^{-1}; *SI Appendix*, Table S1) and land building outpaced land loss on average, leading to net land-area gain at ~570 cm^2/h (Fig. 3*D*). The lobe-averaged model accurately captures the amount of land loss (Eq. **4** in Fig. 3*E*) and the trajectory of the dry land area (Eq. **3** in Fig. 3*D*). The initial, sudden drop in dry delta-plain area (43.5 − 48 h) may reflect transient sedimentation of the trunk channel upstream of the delta lobes—a process that can temporarily increase lobe thickness H and delay avulsion (40), thereby reducing dry-land area (Eqs. **3**–**5**).

The lobe-averaged model reproduces the increase in avulsion frequency (Eq. **5**), which arises because the river responds to rising sea level by partitioning a greater fraction of sediment to delta-plain deposition (~13%, as compared to ~8% during stable sea-level; Fig. 3*F*), which destabilizes channels more quickly (44). In contrast, the landscape-averaged model predicts no land loss (*SI Appendix*, Eq. **S6** in Fig. 3*E*), overestimating the dry-land area and more closely following the trajectory of the total delta plain (Eq. **1** in Fig. 3*D*). This is because the landscape-averaged model does not differentiate between persistent and intermittent land; the area A in Eq. **1** pertains to the delta plain where deposition occurs, and not necessarily the delta plain that is persistently dry. Intermittent land was usually submerged, but was emersed when revisited by the river such that it accreted roughly at pace with persistent land. Thus, the sediment deposited in intermittent zones is a sediment sink not accounted for by landscape-averaged predictions, which leaves less sediment available to build persistently dry land.

More rapid sea-level rise during Phase C ($\sigma^* = 0.33$; Fig. 3*C*) caused more extensive land loss and a long-term reduction in the dry-land area (Fig. 3*A*–*C*). Inactive shorelines retreated a distance of ~45 cm before being replenished by the active channel, resulting in a drowned area of ~2.5 m^2, which was ~50% of the total delta-plain area (Fig. 3*E*). Importantly, despite a fourfold increase in rise rate compared to Phase B, land loss increased by only a factor of 2; this is because avulsions were more frequent ($f_A = 1.0$ [0.6, 2.1] h^{-1}; *SI Appendix*, Table S2), partially mitigating land loss by limiting the duration of sediment starvation. Similar to Phase B, the lobe-averaged model accurately predicts the observed experimental land loss (Eq. **4** in Fig. 3*E*) and the trajectory of dry-land area (Eq. **3** in Fig. 3*D*), whereas the landscape-averaged model overestimates dry-land area by a factor of 2 (Eq. **1** in Fig. 3*D*) and erroneously predicts negligible land loss (*SI Appendix*, Eq. **S6** in Fig. 3*E*). By the end of Phase C, the landscape-averaged model predicts that the delta-plain area should have reached its maximum size in the experiment (~5 m^2); in reality, over half the delta plain had drowned (Fig. 3*D*). By taking the ratio of terms in Eq. **5** (*SI Appendix*, Eqs. **S1**–**S3**), we estimate that ~30% of the sediment supply during Phase C was deposited on the delta plain as a whole (the other 70% was deposited on the delta foreset offshore; Fig. 3*F*). The ~30% provided to the delta plain was split roughly evenly between persistently dry land and intermittent land, such that only ~15% of the total sediment supply contributed to deposition on persistent land. This is only ~8% greater than the amount partitioned to persistent land during Phase B despite a fourfold increase in sea-level rise rate (Fig. 3*F*).

During Phase D, sea-level rise was further increased to exceed the maximum possible sedimentation rate ($\sigma^* = 1.33 > 1$; Eq. **6**; Fig. 3*C*). As a result, shorelines retreated even at the active river mouth; land was lost at a rate of ~9000 cm^2/h, and the delta plain was completely submerged within 2 h (Fig. 3*D*). Both models predict land loss in this phase (Fig. 3*D* and *E*), but the landscape-averaged model overestimates the amount of dry land at any given time, similar to earlier phases. The lobe-averaged model provides reliable estimates, until the point the entire delta was entirely submerged and avulsions ceased. Nearly the entire sediment supply during this phase was partitioned to the delta plain, consistent with previous studies (37, 45), with the majority (~65%) being delivered to intermittent land (Fig. 3*F*)

Discussion and Conclusions

River deltas receive substantial sediment deposition on terrain that is intermittently exposed subaerially as land but is usually submerged. The lobe-averaged model and experimental results demonstrate how, at a given time, the river builds land on the active lobe, and inactive lobes are drowned to an extent that depends on the time since they were last supplied with sediment (Figs. 3*A* and *B* and 4*A*), creating a zone of intermittent land. After avulsion, deposition shifts to a new lobe where intermittent land is replenished with sediment. At the same time, the previously active lobe commences drowning and the zone of intermittent land on the oldest lobes approaches full submergence (Fig. 4*B*). This process continues for each avulsion cycle (Fig. 4*C*), maintaining an approximately constant area of intermittent land delta-wide because the delta is composed of multiple lobes with staggered histories of active sediment supply and inactivity (Fig. 4*A*–*D*). In terms of sediment mass balance, deposition in intermittent zones is a sediment sink that leaves less sediment available to nourish persistently dry land (Fig. 3*F*). In consequence, land loss on deltas is more extensive than predictions from landscape-averaged models (Fig. 3*D* and *E*) that have classically relied on the assumption that all available riverine sediment can be deposited on persistently dry land (i.e., $A = A_{dry}$ in Eq. **2**).

To assess the effect of deltaic avulsions on land loss globally, we revised previous sediment budgets by evaluating Eq. **2** accounting for deposition in both persistent and intermittent land areas ($A = A_{dry} + A_{lost}$) (Fig. 4*E*) using available data (*SI Appendix*). These revised estimates support that deltas are in more danger of land loss than previously anticipated. For example, we find the Mississippi River delta will need more than three times greater sediment supply than previously estimated to sustain its current dry-land area (Fig. 4*E*), an amount totaling $Q_{s,need} = 201$ Gt. This is more than five times the sediment available by some estimates (46), although others have estimated that greater sediment supply is possible (47). Similarly, we estimate that the Orinoco and Parana deltas in South America need roughly triple the sediment than estimated previously to maintain current dry-land area. In Europe, the Rhone and Rhine-Meuse deltas need more than five times the sediment, and the Danube needs more than 10 times the sediment compared to previous estimates—all far beyond the estimated riverine sediment supply available. Not all deltas are predicted to drown; rivers like the Yellow and Brahmaputra have enough sediment to maintain their current land area. The fate of many other deltas is uncertain (Fig. 4*E*) because revised estimates require quantification of the avulsion frequency, which is difficult to constrain and is unavailable for many deltas.

The fate of river deltas depends upon the frequency of river avulsions (Fig. 4*F*). In our experiment, river avulsions occurred more frequently as sea-level rise increased (*SI Appendix*, Table S1), partially mitigating land loss through a negative feedback. As captured in Eq. **4**, as rise rate increases, the rate of land loss

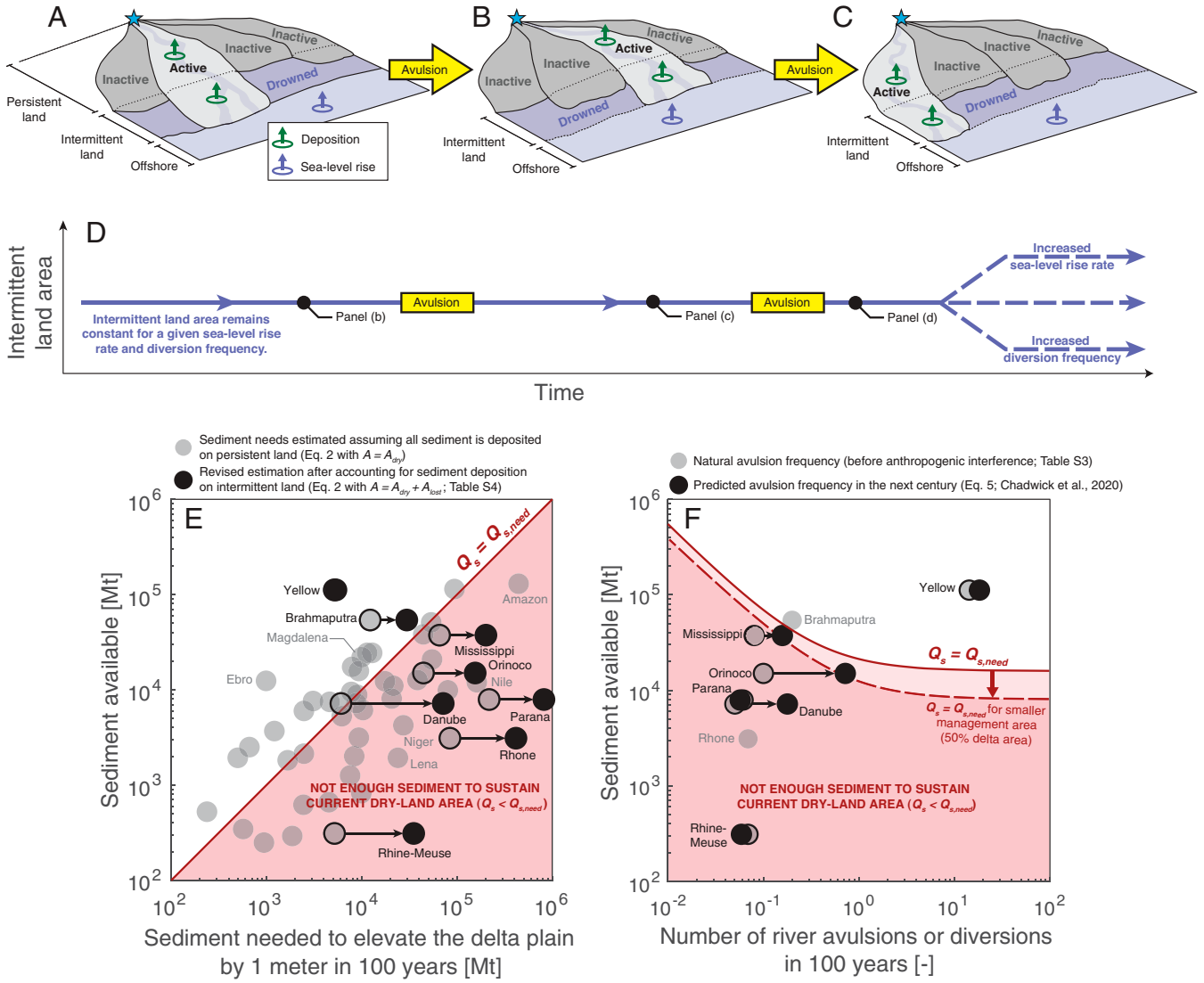

Fig. 4. (*A*–*D*) Schematic of intermittent land dynamics. (*A*) On inactive lobes (dark gray), intermittent land is deprived of riverine sediment and gradually drowns due to sea-level rise (blue arrows). (*B*–*C*) As the river experiences avulsions over time, lobes are periodically reactivated (light gray) and sediment deposition (green arrows) accretes both intermittent land and persistent land. (*D*) The area of intermittent land is persistent until changes in sea-level rise rate or diversion frequency are introduced (Eqs. **3**–**5**). (*E*) Sediment budgets for deltas in the face of 1 m of sea-level rise in the next century. The shaded region highlights conditions where the sediment available is insufficient to sustain the modern delta plain. Gray circles are estimates for different deltas based on the landscape-averaged model (Eq. **2** with $A = A_{dry}$; Giosan et al., ref. 10). Black circles are revised estimates using the lobe-averaged model (Eq. **2** with $A = A_{dry} + A_{lost}$), which accounts for sediment deposition on intermittently drowned land (Eq. **4**; effect indicated by empty black circles and arrows). (*F*) The effect of river diversion frequency on sediment budgets. Boundary of the shaded region was calculated by combining Eqs. **2**–**4** (*SI Appendix*, Eq. **S7**). The dashed red line and arrow show predicted shift in the shaded boundary for management strategies that focus diversion efforts within a smaller, targeted management area covering only 50% of the delta plain. Gray circles show natural diversion frequency before anthropogenic interference, and black circles show predicted diversion frequency in the face of 1 m of sea-level rise over the next century (Eq. **5**). Revised estimates in *E* and model predictions in *F* are not possible for deltas where diversion data are unavailable.

($\frac{\sigma}{S}P$) increases, but at the same time more frequent avulsions reduce the amount of time ($\frac{\eta}{f_A}$) that lobes spend inactive without riverine sediment supply. This change of pace in lobe activity reduces the area of intermittent land and the volume of sediment lost to intermittent land, leading to a relative increase in sediment supply to persistently dry land. As a result, an order-of-magnitude increase in rise rate ($\sigma^* = 0.1$ to 1), like that in our experiment, should incur only a doubling of lost land ($\frac{A_{lost}}{A} = 28\%$ to 60%; Fig. 3*E*). This negative feedback helps mitigate land loss on deltas, which are also expected to avulse more frequently in the coming century (Fig. 4*F*) (37). However, there is a limit to the feedback: If rise rate increases beyond $\sigma^* > 1$ (Eq. **6**), avulsion frequency ceases to naturally increase and land loss accelerates with rise rate (Eq. **4** in Fig. 3*E*). Anthropogenic interference is pushing many deltas beyond this limit (5, 37). For example, the Mississippi was built over the last eight millennia with $\sigma^* \sim 0.3$ (40), but anthropogenic sea-level rise and coastal subsidence may have already forced the Mississippi into $\sigma^* > 1$ conditions (37). Our model suggests that the $\sigma^* > 1$ scenario could render the entire delta plain as intermittent land ($\frac{A_{lost}}{A} = 100\%$; Fig. 3*E*), implying imminent drowning as far as ~500 km inland to the avulsion site near Baton Rouge (21, 38) (Fig. 1*A* and *C*). Where natural avulsions are not sufficient or prevented by manmade infrastructure, mitigating land loss will require frequent engineered diversions.

Our results indicate that sediment supply is most efficiently leveraged as a land-building resource when engineered diversions commit flow to different delta lobes regularly, maintaining an inland zone of persistent dry land similar to natural avulsions (Fig. 4*A*–*D*). Such an approach has already proven successful on

the Yellow River, where four engineered diversions in the past 70 y have facilitated long-term land gains (26, 48). For planning future engineered diversions on deltas under accelerating sea-level rise (5), the lobe-averaged model (Eqs. **3**–**5**) provides a framework to optimize sediment resources and mitigate land loss. Without avulsions or diversions, anthropogenic increases to relative sea-level rise (σ) will result in proportional increases in land loss (A_{lost}; Eq. **4**). For example, in a scenario where rise rate doubles, diversion frequency (f_A) should at least be doubled to prevent further land loss. More frequent diversions provide further benefits by reducing the area of intermittent land in favor of persistently dry land, and effectively maximizing sediment supply to persistent land (Fig. 4*F*) (*SI Appendix*). Long-lived, regularly scheduled diversions offer promise for some deltas; on the Mississippi and Orinoco, for instance, the existing dry-land area can be maintained with the available sediment supply if diversions occur at least once per century and once per decade, respectively (Fig. 4*F*). In contrast, on the Parana, Danube, and Rhine-Meuse, more frequent river diversions are not enough; more sediment must be made available for the existing land area to remain persistently dry (Fig. 4*F*).

Where existing dry land cannot be saved, smaller-scale diversions can also improve the outlook for prioritized coastal zones. Plans for the Mississippi (11, 12, 34) call for focused diversions within smaller portions of the delta compared to what has historically been replenished. Reducing the size of the management area effectively reduces sediment supply requirements for maintaining land persistently dry therein (Fig. 4*F*; *SI Appendix*). But this plan comes with the trade-off that intermittent land outside the management area will become permanently lost if it is not supplied with sediment. Planned land loss can be cost-effective depending on the delta (34, 49) by creating new wetland ecosystems that capture biogenic and offshore sediment in residual channels (15–17) and providing storm dissipation for prioritized zones inland (11, 27). Partial diversions can also be effective, as demonstrated by the Atchafalaya diversion of the Mississippi River that has persisted since 1963 (Fig. 1*A*) (30–32). Partial diversions increase the number of simultaneous active lobes, which can produce local land gains (e.g., the Wax Lake subdelta; Lobe 6 in Fig. 1*C*) (12, 32), but can also exacerbate land loss in other areas with reduced sediment supply (e.g., the Birdfoot subdelta; Lobe 5 in Fig. 1*C*) (50, 51). Even for smaller-scale and partial diversion strategies, committed decisions need to be made as to where and how much land should be prioritized for management through diversions.

Once a management zone is adopted, efforts must commit to this zone with regular, long-lived diversions in order to fully leverage sediment resources. Temporary opening of flood byways provides only short-term land gains (52, 53); if these areas are left to drown in later decades then the sediment resources diverted there represent a sunk cost. With the same sediment supply, larger management areas can be maintained using more frequent diversions because this minimizes the zone of intermittent land (Fig. 4*A*–*D*), but frequent diversions also introduce engineering costs, relocation efforts, and ecosystem pressures (11, 25, 26). Economic analysis suggests that the benefits of frequent diversions can outweigh the costs, even when considering the active lobe alone (25). Diversions will never be frequent enough to fully eliminate intermittent land; doing so would require an infinite diversion frequency (i.e., $A_{lost} \to 0$ when $f_A \to \infty$ in Eq. **5**). With this in mind, management plans need to decide upon a target, acceptable amount of land loss (A_{lost}) and implement diversions at a scheduled frequency (f_A) that meets this target. Diversions need to reoccur indefinitely—just like natural avulsions—or else inactive zones will drown and sediment previously delivered there will be a wasted resource. Furthermore, diversions should be placed to minimize deposition on intermittent land near the coast, prioritizing deposition in inland areas that can be maintained indefinitely. Doing so will make efficient use of riverine sediment as a natural resource to restore sinking land, and strike a balance between coastal sustainability and river stability (27) that will be crucial for the survival of coastal communities in the coming century.

Materials and Methods

In the laboratory experiment, overhead cameras captured plan-view imagery of the delta every minute. The water was dyed fluorescent green, which allowed visual distinction between subaerial and submerged land under ultraviolet light fixtures. We manually mapped the extent of subaerial and submerged land (Fig. 3*A*) and identified avulsions where and when the flow established a new channel that captured the majority of flow (Fig. 3*B*) (44, 54). For each avulsion, we measured the avulsion length (L_A) and avulsion frequency ($f_A \equiv 1/T_A$, where T_A is the time since the previous avulsion). Further details regarding the experimental setup can be found in Ganti et al. (54) and the *SI Appendix*.

For both the experiment and field data, the lobe-averaged model (Eqs. **3**–**5**) was implemented by solving Eq. **5** for f_A, using an iterative scheme and input estimates of Q_s, c_0, L_A, B, H, S, N, and σ (37), and plugging the result into Eqs. **4** and **5** to determine A_{dry} and A_{lost} (*SI Appendix*, Tables S2–S4). For simplicity we adopted a characteristic number of lobes $N = 5 \pm 1$, consistent with field observations (20, 21, 29, 55) and experiments (56–58), and propagated uncertainty associated with lobe number to land-loss predictions (*SI Appendix*). Landscape-averaged model predictions were reported by Giosan et al. (10) for field data, and for the experiment were determined by numerically solving Eq. **1** for A and performing a scaling analysis to estimate A_{lost} (*SI Appendix*). The fraction of sediment partitioned to persistent dry land, intermittent land, and farther offshore (Fig. 3*F*) was estimated by taking the ratio of terms in Eq. **5** (*SI Appendix*).

Data Availability. The data and MATLAB codes underlying this study are publicly available and were deposited in the SEAD Internal Repository (https://doi.org/10.26009/s0A0QNM6) (59).

ACKNOWLEDGMENTS. We thank Vamsi Ganti for useful discussions and acknowledge NSF Grant EAR 1427262 and the Resnick Sustainability Institute at the California Institute of Technology for support.

1. C. J. Vörösmarty *et al.*, Battling to save the world's river deltas. *Bull. At. Sci.* **65**, 31–43 (2009).
2. J. P. M. Syvitski, Y. Saito, Morphodynamics of deltas under the influence of humans. *Global Planet. Change* **57**, 261–282 (2007).
3. J. P. M. Syvitski *et al.*, Sinking deltas due to human activities. *Nat. Geosci.* **2**, 681–686 (2009).
4. J. P. Ericson, C. J. Vörösmarty, S. L. Dingman, L. G. Ward, M. Meybeck, Effective sea-level rise and deltas: Causes of change and human dimension implications. *Global Planet. Change* **50**, 63–82 (2006).
5. J. A. Church, N. J. White, A 20th century acceleration in global sea-level rise. *Geophys. Res. Lett.* **33**, L01602 (2006).
6. J. D. Milliman, B. U. Haq, *Sea-Level Rise and Coastal Subsidence: Causes, Consequences, and Strategies* (Springer Science & Business Media, 2013).
7. R. H. Kesel, The decline in the suspended load of the lower Mississippi River and its influence on adjacent wetlands. *Environ. Geol. Water Sci.* **11**, 271–281 (1988).
8. S. Temmerman, M. L. Kirwan, Building land with a rising sea. *Science* **349**, 588–589 (2015).
9. J. P. M. Syvitski, Deltas at risk. *Sustain. Sci.* **3**, 23–32 (2008).
10. L. Giosan, J. Syvitski, S. Constantinescu, J. Day, Climate change: Protect the world's deltas. *Nature* **516**, 31–33 (2014).
11. Coastal Protection and Restoration Authority of Louisiana, Integrated ecosystem restoration and hurricane protection: Louisiana's comprehensive master plan for a sustainable coast. State of Louisiana: Baton Rouge, LA (2007).
12. W. Kim, D. Mohrig, R. R. Twilley, C. Paola, G. Parker, Is it feasible to build new land in the Mississippi River delta? *Eos (Wash. D.C.)* **90**, 373–374 (2009).
13. D. J. Jerolmack, Conceptual framework for assessing the response of delta channel networks to Holocene sea level rise. *Quat. Sci. Rev.* **28**, 1786–1800 (2009).
14. C. Paola *et al.*, Natural processes in delta restoration: Application to the Mississippi Delta. *Annu. Rev. Mar. Sci.* **3**, 67–91 (2011).

15. C. D. Woodroffe *et al.*, Mangrove sedimentation and response to relative sea-level rise. *Annu. Rev. Mar. Sci.* **8**, 243–266 (2016).
16. L. G. Ward, B. J. Zaprowski, K. D. Trainer, P. T. Davis, Stratigraphy, pollen history and geochronology of tidal marshes in a Gulf of Maine estuarine system: Climatic and relative sea level impacts. *Mar. Geol.* **256**, 1–17 (2008).
17. A. Finotello, N. Lentsch, C. Paola, Experimental delta evolution in tidal environments: Morphologic response to relative sea-level rise and net deposition. *Earth Surf. Process. Landf.* **44**, 2000–2015 (2019).
18. L. Giosan *et al.*, River delta morphodynamics: Examples from the Danube Delta. *SEPM Spec. Publ.* **83**, 393–412 (2005).
19. H. Wang, Z. Yang, G. Li, W. Jiang, Wave climate modeling on the abandoned Huanghe (Yellow River) delta lobe and related deltaic erosion. *J. Coast. Res.* **22**, 906–918 (2006).
20. J. Pang, S. Si, The estuary changes of Huanghe River I. Changes in modern time. *Oceanol. Limnol. Sin.* **10**, 136–142 (1979).
21. J. M. Coleman, H. H. Roberts, G. W. Stone, Mississippi River delta: An overview. *J. Coast. Res.* **14**, 698–716 (1998).
22. R. Slingerland, N. D. Smith, River avulsions and their deposits. *Annu. Rev. Earth Planet. Sci.* **32**, 257–285 (2004).
23. D. J. Jerolmack, J. B. Swenson, Scaling relationships and evolution of distributary networks on wave-influenced deltas. *Geophys. Res. Lett.* **34**, L23402 (2007).
24. V. Ganti, Z. Chu, M. P. Lamb, J. A. Nittrouer, G. Parker, Testing morphodynamic controls on the location and frequency of river avulsions on fans versus deltas: Huanghe (Yellow River), China. *Geophys. Res. Lett.* **41**, 7882–7890 (2014).
25. A. J. Moodie, J. A. Nittrouer, Optimized river diversion scenarios promote sustainability of urbanized deltas. *Proc. Natl. Acad. Sci. U.S.A.* **118**, e2101649118 (2021).
26. B. N. Carlson *et al.*, Impacts of engineered diversions and natural avulsions on delta-lobe stability. *Geophys. Res. Lett.* **48**, e2021GL092438 (2021).
27. P. Passalacqua, L. Giosan, S. Goodbred, I. Overeem, Stable ≠ sustainable: Delta dynamics versus the human need for stability. *Earth's Future* **9**, e2021EF002121 (2021).
28. Louisiana Coastal Wetlands Conservation and Restoration Task Force and Wetlands Conservation and Restoration Authority, *Coast 2050: Toward a Sustainable Coastal Louisiana* (Louisiana Department of Natural Resources, Baton Rouge, LA, 1998).
29. Z. X. Chu, X. G. Sun, S. K. Zhai, K. H. Xu, Changing pattern of accretion/erosion of the modern Yellow River (Huanghe) subaerial delta, China: Based on remote sensing images. *Mar. Geol.* **227**, 13–30 (2006).
30. J. Mossa, The changing geomorphology of the Atchafalaya River, Louisiana: A historical perspective. *Geomorphology* **252**, 112–127 (2016).
31. H. H. Roberts, Delta switching: Early responses to the Atchafalaya River diversion. *J. Coast. Res.* **14**, 882–899 (1998).
32. H. H. Roberts, J. M. Coleman, S. J. Bentley, N. Walker, An embryonic major delta lobe: A new generation of delta studies in the Atchafalaya-Wax Lake Delta system. *Gulf Coast Assoc. Geol. Soc. Trans.* **53**, 690–703 (2003).
33. Y. Chen, J. P. M. Syvitski, S. Gao, I. Overeem, A. J. Kettner, Socio-economic impacts on flooding: A 4000-year history of the Yellow River, China. *Ambio* **41**, 682–698 (2012).
34. M. A. Kenney *et al.*, Cost analysis of water and sediment diversions to optimize land building in the Mississippi River delta. *Water Resour. Res.* **49**, 3388–3405 (2013).
35. V. Ganti, M. P. Lamb, A. J. Chadwick, Autogenic erosional surfaces in fluvio-deltaic stratigraphy from floods, avulsions, and backwater hydrodynamics. *J. Sediment. Res.* **89**, 815–832 (2019).
36. D. Mohrig, P. L. Heller, W. J. Lyons, Interpreting avulsion process from ancient alluvial sequences: Guadalope-Matarranya system (northern Spain) and Wasatch Formation (western Colorado). *GSA Bull.* **112**, 1787–1803 (2000).
37. A. J. Chadwick, M. P. Lamb, V. Ganti, Accelerated river avulsion frequency on lowland deltas due to sea-level rise. *Proc. Natl. Acad. Sci. U.S.A.* **117**, 17584–17590 (2020).
38. P. Chatanantavet, M. P. Lamb, J. A. Nittrouer, Backwater controls of avulsion location on deltas. *Geophys. Res. Lett.* **39**, L01402 (2012).
39. P. Chatanantavet, M. P. Lamb, Sediment transport and topographic evolution of a coupled river and river plume system: An experimental and numerical study. *J. Geophys. Res. Earth Surf.* **119**, 1–20 (2014).
40. A. J. Chadwick, M. P. Lamb, Climate-change controls on river delta avulsion location and frequency. *J. Geophys. Res. Earth Surf.* **126**, e2020JF005950 (2021).
41. A. Piliouras, W. Kim, B. Carlson, Balancing aggradation and progradation on a vegetated delta: The importance of fluctuating discharge in depositional systems. *J. Geophys. Res. Earth Surf.* **122**, 1882–1900 (2017).
42. R. L. Caldwell *et al.*, A global delta dataset and the environmental variables that predict delta formation on marine coastlines. *Earth Surf. Dyn.* **7**, 773–787 (2019).
43. W. Kim, C. Paola, J. B. Swenson, V. R. Voller, Shoreline response to autogenic processes of sediment storage and release in the fluvial system. *J. Geophys. Res. Earth Surf.* **111**, 1–15 (2006).
44. M. Bryant, P. Falk, C. Paola, Experimental study of avulsion frequency and rate of deposition. *Geology* **23**, 365 (1995).
45. J. Martin, B. Sheets, C. Paola, D. Hoyal, Influence of steady base-level rise on channel mobility, shoreline migration, and scaling properties of a cohesive experimental delta. *J. Geophys. Res.* **114**, F03017 (2009).
46. J. D. Milliman, J. P. M. Syvitski, Geomorphic/tectonic control of sediment discharge to the ocean: The importance of small mountainous rivers. *J. Geol.* **100**, 525–544 (1992).
47. J. A. Nittrouer, E. Viparelli, Sand as a stable and sustainable resource for nourishing the Mississippi River delta. *Nat. Geosci.* **7**, 350–354 (2014).
48. Y. Liu, X. Li, X. Hou, Spatiotemporal changes to the river channel and shoreline of the yellow river delta during a 40-year period (1976–2017). *J. Coast. Res.* **36**, 128 (2019).
49. M. A. Allison, E. A. Meselhe, The use of large water and sediment diversions in the lower Mississippi River (Louisiana) for coastal restoration. *J. Hydrol. (Amst.)* **387**, 346–360 (2010).
50. J. W. Day *et al.*, Pattern and process of land loss in the Mississippi delta: A spatial and temporal analysis of wetland habitat change. *Estuaries* **23**, 425 (2000).
51. B. R. Couvillion *et al.*, Land area change in coastal Louisiana from 1932 to 2010. *U.S. Geol. Surv. Sci. Investig. Map* **3164**, 12 (2011).
52. J. A. Nittrouer *et al.*, Mitigating land loss in coastal Louisiana by controlled diversion of Mississippi River sand. *Nat. Geosci.* **5**, 534–537 (2012).
53. W. Kim, Geomorphology: Flood-built land. *Nat. Geosci.* **5**, 521–522 (2012).
54. V. Ganti, A. J. Chadwick, H. J. Hassenruck-Gudipati, B. M. Fuller, M. P. Lamb, Experimental river delta size set by multiple floods and backwater hydrodynamics. *Sci. Adv.* **2**, e1501768 (2016).
55. H. H. Roberts, Dynamic changes of the Holocene Mississippi River delta plain: The delta cycle. *J. Coast. Res.* **13**, 605–627 (1997).
56. B. N. Carlson, A. Piliouras, T. Muto, W. Kim, Control of basin water depth on channel morphology and autogenic timescales in deltaic systems. *J. Sediment. Res.* **88**, 1026–1039 (2018).
57. M. D. Reitz, D. J. Jerolmack, J. B. Swenson, Flooding and flow path selection on alluvial fans and deltas. *Geophys. Res. Lett.* **37**, L06401 (2010).
58. A. J. Chadwick, M. P. Lamb, A. J. Moodie, G. Parker, J. A. Nittrouer, Origin of a preferential avulsion node on lowland river deltas. *Geophys. Res. Lett.* **46**, 4267–4277 (2019).
59. A.J. Chadwick, S. Steele, J. Silvestre, M.P. Lamb, More extensive land loss expected on coastal deltas due to rivers jumping course during sea-level rise. SEAD. https://doi.org/10.26009/s0A0QNM6. Deposited 10 May 2022.